7311 Characterization of PERK-Positive Polyploid-Like Breast Cancer Cells and Their Association with Unfolded Protein Response Signatures

Luis del Pozo-Yauner[1], Veronica Ramirez-Alcantara[2], Elba A. Turbat-Herrera[3], Hector Chavarria Bernal[1], Maha Babker[1], Huseyin Kilic[1], Rosetta Campbell[1], Bahaaeldin Youssef[1], Ajay Singh[4], Julio Isael Perez-Carreon[5], Wei Yang[6], Guillermo A. Herrera[1]. [1]Pathology, University of South Alabama College of Medicine, Mobile, AL; [2]USA Health Mitchell Cancer Institute, Mobile, AL; [3]4SOM-Cell and Molecular Biology, University of Mississippi Medical Center and Cancer Center and Research Institute, Jackson, MS, [5]National Institute of Genomic Medicine, Mexico City, Mexico,[6]Bruker Spatial Biology, Seattle, WA.

Background

Endoplasmic reticulum (ER) stress is a common feature of breast cancer and activates the unfolded protein response (UPR) through three major sensors: PERK, IRE1α, and ATF6. Persistent UPR signaling helps tumor cells adapt to hypoxia, nutrient deprivation, and other microenvironmental stressors [1,2]. PERK is a key UPR effector that signals through the eIF2α/ATF4 axis to regulate cellular stress adaptation. In breast cancer, increased PERK activity has been associated with higher histologic grade, aggressive clinicopathologic features, and poorer outcomes [3,4]. Experimental studies further indicate that PERK-driven signaling promotes aggressive tumor cell programs, including hypoxia-associated migration and invasion, as well as maintenance of stem-like cell states, supporting a role for PERK in breast cancer plasticity and progression [2,5]. In a previous study of high-grade serous ovarian carcinoma, we identified a small subset of cancer cells with strong phospho-PERK (pPERK) expression, some of which displayed polyploid-like or atypical mitotic morphology (Figure 1). In a subsequent study, we observed cells with similar features in breast cancer (BC), raising the possibility that they represent a biologically distinct, stress-adapted population associated with active UPR signaling. These observations provided the rationale to investigate the frequency of PERK-positive breast cancer cells, their association with UPR activation, and the molecular features of tumors enriched in these cells.

Objective

This study aimed to determine the frequency of PERK-positive cells in BC tumors, evaluate their association with UPR activation, and identify transcriptomic and proteomic features associated with tumors containing these cells.

Study design and cohort.

Formalin-fixed, paraffin-embedded (FFPE) tissues from 131 breast cancer (BC) patients (96 TNBC and 35 non-TNBC) were analyzed by immunohistochemistry (IHC) using a rabbit polyclonal anti-phospho-PERK (Thr982) antibody (Invitrogen, Cat. No. PA5-102853). For the purposes of this study, pPERK-positive BC cells were defined as tumor cells showing strong (3+) cytoplasmic and nuclear phospho-PERK staining. BC tumors were stratified according to the number of pPERK-positive cells identified in three different tumor regions examined at **200× magnification** into three groups: **abundant** (≥30 cells), **scarce** (≤10 cells), and **absent** (none).

Clinical variables and stratification.

Race/ethnicity, age at diagnosis, biomarker status (ER, PR, HER2, and Ki-67), histologic grade, and pathologic stage were obtained from the electronic medical record. Breast cancer molecular subtypes were assigned according to standard clinical classification (Luminal A, Luminal B, HER2-enriched, and triple-negative breast cancer [TNBC]) based on receptor status documented in pathology reports.

nCounter multiomics analysis.

Gene expression and protein profiling were performed using the nCounter platform (NanoString Technologies, Seattle, WA). Twenty-one breast cancer samples and three normal breast tissues were analyzed using the Breast Cancer 360 (BC360) transcriptomic panel, which measures 776 genes spanning 23 major breast cancer pathways and biologic processes, together with the nCounter Multiomics Protein Core, nCounter Multiomics Immune Pathways Protein, and nCounter Multiomics Tumor Signaling Protein panels, comprising a total of 545 protein-related analytes. This platform enables direct digital quantification of RNA transcripts and proteins without amplification, allowing integrated assessment of oncogenic pathways, immune signatures, and the tumor microenvironment.

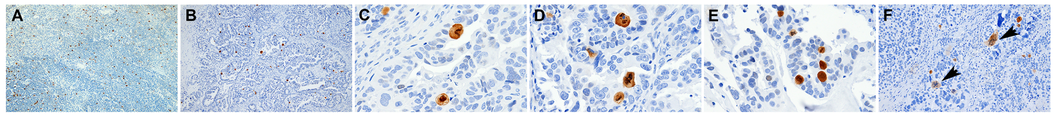

Figure 1. Immunohistochemical detection of phospho-PERK in high-grade serous ovarian carcinoma. Low-magnification images in **A** and **B** show strongly positive tumor cells distributed throughout the tumor. **C** and **E** show examples of these cells at higher magnification. F shows phospho-PERK-positive cells with polyploid giant cancer cell-like morphology. Immunostaining was performed using a rabbit polyclonal anti-phospho-PERK (Thr982) antibody (Invitrogen, Cat. No. PA5-102853), followed by an HRP-conjugated goat anti-rabbit secondary antibody.

Table 1. Clinicopathologic features of breast cancer cases analyzed by nCounter multiomics. Breast cancer samples were stratified by the number of strongly phospho-PERK-positive tumor cells and compared according to age, race/ethnicity, receptor status, subtype, proliferation index, pathologic stage, treatment response, metastatic status, and vital status.

Sample ID	pPERK+ cells	Race / Ethnicity	Age at diagnosis	ER	PR	HER2/neu	Ki67 (%)	Subtype	Response to neoadjuvant therapy	Histological grade	Pathologic stage (pTNM)	Number of positive lymph nodes	Lymphovascular invasion	Distant metastasis / Recurrence status	Vital status
25-01	≤10	NHW	56	Positive (68%)	Negative	Negative	28.0	Luminal A	NA	3	pT2(3) pN1a	1	Present	No	Alive
25-06	≤10	Other	47	Positive (87%)	Positive (89%)	Negative	5.0	Luminal A	NA	1	pT1c pN1a	1	Present	No	Alive
25-08	≤10	NHW	85	Negative	Negative	Negative	43.5	TNBC	NA	NA	NA	NA	No determined	Metastatic unknown primary	Alive
25-09	≤10	NHW	43	Negative	Negative	Negative	75.5	TNBC	Minimal response	3	ypT2 ypN1a	2	Present	No	Alive
25-13	≥30	NHW	62	Positive (95%)	Positive (93%)	Negative	17.0	Luminal A	NA	3	pT2(m) pN0	0	No determined	No	Deceased
25-19	≥30	NHW	60	Positive (100%)	Positive (23%)	Negative	30.0	Luminal A	NA	2	pT4b pN2a	4	Present	Ulceration of skin	Deceased
25-11	≥30	NHW	58	Negative	Negative	Negative	76.8	TNBC	No response	3	ypT3(m) ypN1a	2	Present	No	Deceased
25-12	≥30	NHB/AA	58	Negative	Negative	Negative	42.1	TNBC	NA	3	pT1c pN0sn-i	0	No determined	No	Alive
25-14	≥30	NHB/AA	54	Negative	Negative	Negative	19.6	TNBC	NA	3	NA	NA	No determined	NA	Alive
25-15	≥30	NHB/AA	56	Negative	Negative	Negative	47.0	TNBC	No response	3	ypT2 ypN0	0	Present	No	Deceased
25-16	≥30	NHW	35	Negative	Negative	Negative	77.2	TNBC	NA	3	NA	NA	No determined	Axillary LN	Deceased
25-17	≥30	NHB/AA	49	Negative	Negative	Negative	76.9	TNBC	No response	3	ypT3 ypN1a	1	Present	NA	Alive
25-18	≥30	NHB/AA	45	Negative	Negative	Negative	47.9	TNBC	No response	3	ypT2 ypN0	0	No identified	No	Alive
25-20	≥30	NHB/AA	61	Negative	Negative	Negative	63.7	TNBC	NA	3	NA	NA	No determined	NA	Deceased
25-21	≥30	NHB/AA	31	Negative	Negative	Negative	60.2	TNBC	No known presurgical treatment	3	pT2 pN0	0	Present	No	Alive
25-10	No	NHB/AA	33	Negative	Negative	Negative	66.0	TNBC	Probable response	3	pyT3 ypN0	0	No identified	No	Alive
25-02	No	NHB/AA	54	Positive (99%)	Positive (7%)	Negative	21.0	Luminal A	NA	3	pT1c pN1a	1	No identified	No	Alive
25-03	No	NHB/AA	54	Positive	Positive	Negative	21.0	Luminal A	NA	3	pT1c pN1a	1	No determined	No	Alive
25-04	No	NHW	58	Positive (96%)	Positive (94%)	Negative	5.9	Luminal A	NA	2	pT1c pN1a	1	No identified	NA	Alive
25-07	No	NHB/AA	71	Positive (96%)	Positive (15%)	Negative	9.0	Luminal A	NA	2	pT3 pN1a	1	No identified	No	Deceased
25-05	No	NHW	65	Negative	Negative	Negative	69.0	TNBC	NA	3	pT2 pN0	0	Present	Recurrence	Deceased

Results

Immunohistochemistry identified a distinct subpopulation of breast cancer cells with strong phospho-PERK expression, some showing atypical mitotic features and polyploid giant cancer cell-like morphology (Figure 2). These cells were more frequently associated with TNBC. Based on phospho-PERK staining, 21 tumors were selected for nCounter multiomics analysis, including tumors with abundant strongly positive cells, tumors with few or none, and 3 normal breast tissues. Transcriptomic heatmaps separated normal breast tissue from tumor samples and suggested that tumors enriched in strongly phospho-PERK-positive cells share a partially distinct molecular profile. This pattern was more evident in transcriptomics than in proteomics (Figure 3). Compared with tumors lacking abundant phospho-PERK-positive cells and with normal breast tissue, tumors with abundant strongly positive cells showed increased expression of genes linked to proliferation, stress adaptation, and aggressive behavior, including SLPI, PHGDH, SPP1, KIFC1, CDK1, RRM2, TOP2A, and BIRC5. They also showed reduced expression of genes associated with differentiation, metastasis suppression, or immune surveillance, including LIFR, SPRY2, CXCR6, and CD8A (Figure 4-6). At the protein level, differences between tumor groups were more limited, but tumors with abundant strongly phospho-PERK-positive cells still showed increased expression of proteins related to proliferation, survival, angiogenesis, and stress responses, including PCNA, AKT, VEGF receptor 1, PARP1, Chk2, ATR phospho-S428, and Hsp90. Overall, the integrated data supports an association between abundant strongly phospho-PERK-positive breast cancer cells and a molecular phenotype characterized by unfolded protein response activation, proliferative signaling, metabolic reprogramming, and features consistent with aggressive tumor behavior.

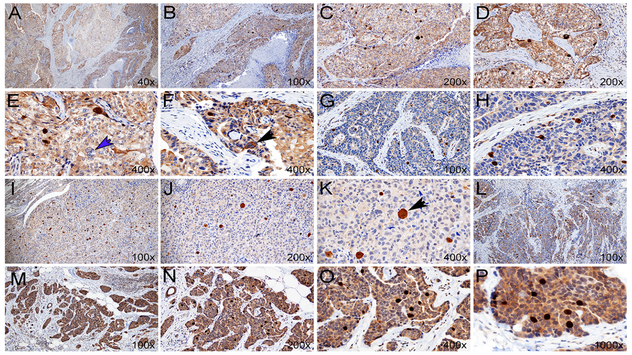

Figure 2. Representative phospho-PERK immunohistochemistry in breast cancers with ≥30 strongly positive tumor cells. Panels **A–F** show case **25-15, G–H** case **25-12, I–K** case **25-11**, L case **25-21,** and **M–P** case **25-16.** These tumors show strongly phospho-PERK-positive cells distributed throughout the tumor, similar to the pattern observed in HGSOC. Total magnification is shown in the lower-right corner. The **blue arrow in E** indicates a polyploid giant cancer cell-like cell that is negative for phospho-PERK, whereas the **black arrows in F and K** indicate polyploid giant cancer cell-like cells that are strongly positive for phospho-PERK. Staining was performed with a rabbit polyclonal anti-phospho-PERK (Thr982) antibody (Invitrogen, Cat. No. PA5-102853) and an HRP-conjugated goat anti-rabbit secondary antibody.

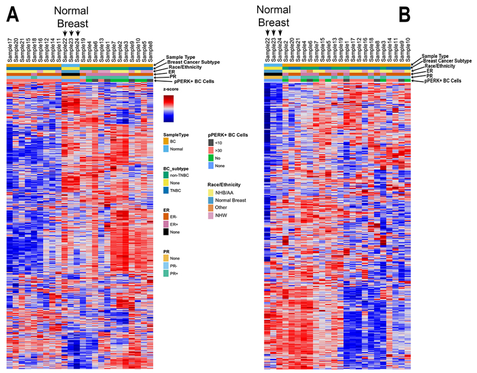

Figure 3. Transcriptomic (A) and proteomic (B) heatmaps of breast cancer and normal breast samples analyzed by nCounter multiomics. Columns correspond to samples and rows to molecular features. Annotation bars indicate phospho-PERK-positive cell category, PR, ER, race/ethnicity, subtype, and sample type. Normal breast samples **(22, 23, 24)** are marked by arrows. Values are displayed as z-scores.

Table 2. Selected differentially expressed genes supporting an aggressive molecular phenotype in breast cancers enriched in strongly phospho-PERK-positive cells. Genes were selected from BH-significant comparisons involving tumors with **≥30 strongly phospho-PERK-positive cells** because their expression patterns are consistent with increased proliferation, metabolic and stress adaptation, treatment resistance, invasion, metastasis, or reduced antitumor immune surveillance.

Gene	BH-significant comparison(s) in ≥30 group	Potential implication in breast cancer pathogenesis
PHGDH	≥30 vs ≤10 (Up, log2FC 2.42, adj p 0.03359); ≥30 vs No (Up, log2FC 2.12, adj p 0.01383)	Serine-synthesis and metabolic-stress adaptation; can support tumor growth and therapy resistance.
CD24	≥30 vs ≤10 (Up, log2FC 2.05, adj p 0.03708)	Cell-surface adhesion/immune-evasion marker; associated in some breast cancer contexts with aggressive behavior and dissemination.
E2F5	≥30 vs ≤10 (Up, log2FC 1.72, adj p 0.0485)	Cell-cycle transcription factor; consistent with proliferative drive.
TRIP13	≥30 vs No (Up, log2FC 1.55, adj p 0.01135)	Chromosome-segregation/DNA-damage response factor; linked to aggressive behavior and anticancer drug resistance.
ATAD2	≥30 vs No (Up, log2FC 1.06, adj p 0.01151); ≥30 vs Normal B (Up, log2FC 2.34, adj p 0.0006898)	Chromatin regulator; associated with proliferation, migration, invasion, and poor prognosis in breast cancer.
SKP2	≥30 vs No (Up, log2FC 1.08, adj p 0.01971)	Cell-cycle and survival regulator; promotes proliferation and has been linked to invasion and poor outcome.
MELK	≥30 vs No (Up, log2FC 1.41, adj p 0.02489)	Kinase associated with aggressive growth and treatment resistance programs.
CCNE2	≥30 vs No (Up, log2FC 1.13, adj p 0.02867); ≥30 vs Normal B (Up, log2FC 2.71, adj p 0.00128)	G1/S cell-cycle progression; supports proliferation and has been associated with aggressive disease.
CDC25C	≥30 vs No (Up, log2FC 1.01, adj p 0.03328); ≥30 vs Normal B (Up, log2FC 1.49, adj p 0.02599)	Cell-cycle checkpoint phosphatase; consistent with mitotic activation and proliferation.
NUF2	≥30 vs No (Up, log2FC 1.39, adj p 0.03931); ≥30 vs Normal B (Up, log2FC 2.56, adj p 0.009158)	Kinetochore/mitotic progression factor; supports proliferative capacity.
SLPI	≥30 vs No (Up, log2FC 4.4, adj p 0.006283)	Secreted factor linked to breast cancer progression and metastasis, especially in aggressive disease.
ENO1	≥30 vs No (Up, log2FC 1.59, adj p 0.001425)	Glycolytic/metabolic adaptation factor; can support stress tolerance and aggressive tumor behavior.
KIFC1	≥30 vs Normal B (Up, log2FC 5.69, adj p 0.0004311)	Centrosome-clustering motor protein; linked to aggressive breast cancer, survival under mitotic stress, and therapy resistance.
CDK1	≥30 vs Normal B (Up, log2FC 3.1, adj p 0.0005484)	Core mitotic kinase; indicates strong proliferative activity.
RRM2	≥30 vs Normal B (Up, log2FC 2.86, adj p 0.00128)	Nucleotide synthesis/DNA replication; supports proliferation and therapy resistance.
BIRC5	≥30 vs Normal B (Up, log2FC 2.78, adj p 0.001428)	Anti-apoptotic survivin pathway; associated with poor prognosis and treatment resistance.
TOP2A	≥30 vs Normal B (Up, log2FC 3.07, adj p 0.003416)	DNA topology/replication factor; marker of highly proliferative tumors.
MKI67	≥30 vs Normal B (Up, log2FC 2.32, adj p 0.00533)	Canonical proliferation marker.
CEP55	≥30 vs Normal B (Up, log2FC 2.46, adj p 0.001422)	Cytokinesis regulator; linked to aggressive growth.
PRC1	≥30 vs Normal B (Up, log2FC 1.84, adj p 0.002128)	Mitotic spindle/cytokinesis regulator; consistent with proliferative activation.
CENPF	≥30 vs Normal B (Up, log2FC 2.85, adj p 0.003658)	Mitotic progression/chromosome segregation; associated with aggressive proliferation.
DLGAP5	≥30 vs Normal B (Up, log2FC 3.86, adj p 0.003541)	Spindle-associated mitotic regulator; linked to rapid cell division.
ANLN	≥30 vs Normal B (Up, log2FC 1.96, adj p 0.005749)	Actin-binding cytokinesis regulator; associated with proliferation and invasion.
FAM83D	≥30 vs Normal B (Up, log2FC 3.23, adj p 0.005908)	Mitotic spindle regulator; associated with breast cancer progression.
SPP1	≥30 vs Normal B (Up, log2FC 5.74, adj p 0.00134)	Osteopontin; promotes tumor recurrence, macrophage recruitment, invasion, and metastasis.
LIFR	≥30 vs ≤10 (Down, log2FC -1.43, adj p 0.02478); ≥30 vs No (Down, log2FC -1.38, adj p 0.00448); ≥30 vs Normal B (Down, log2FC -3.19, adj p 0.0001538)	Metastasis suppressor; reduced expression is consistent with enhanced metastatic potential.
SPRY2	≥30 vs Normal B (Down, log2FC -2.71, adj p 0.0001369)	Negative regulator of RTK/MAPK signaling; reduced expression is consistent with loss of growth-control and worse prognosis.
CXCR6	≥30 vs ≤10 (Down, log2FC -1.33, adj p 0.02277); ≥30 vs No (Down, log2FC -2.07, adj p 0.0001634); ≥30 vs Normal B (Down, log2FC -1.72, adj p 0.00533)	Marker of tumor-resident/antitumor T-cell activity; reduced expression may reflect weaker immune surveillance.
CD8A	≥30 vs No (Down, log2FC -1.74, adj p 0.0001634); ≥30 vs Normal B (Down, log2FC -1.12, adj p 0.02452)	Cytotoxic T-cell marker; reduced expression is consistent with lower antitumor immune infiltration.

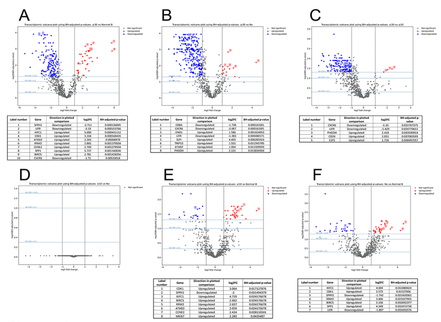

Figure 4. Transcriptomic volcano plots comparing breast cancers stratified by the abundance of strongly phospho-PERK-positive cells and normal breast tissue. Comparisons shown are **A**, >30 vs Normal B; **B**, >30 vs No; **C**, >30 vs <10; **D**, <10 vs No; **E**, <10 vs Normal B; and **F**, No vs Normal B. The x-axis represents log2 fold change and the y-axis −log10(BH-adjusted p-value). Red, blue, and dark gray dots indicate upregulated, downregulated, and non-significant genes, respectively. Numbered labels mark selected differentially expressed genes, which are identified in the tables beneath each panel.

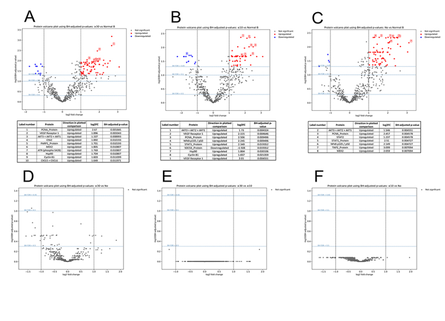

Figure 5. Proteomic volcano plots comparing breast cancers with >30, <10, or no strongly phospho-PERK-positive cells and normal breast tissue. Panels show comparisons of **A**, >30 vs Normal B; **B**, <10 vs Normal B; **C**, No vs Normal B; **D**, >30 vs No; **E**, >30 vs <10; and **F**, <10 vs No. The x-axis shows log2 fold change and the y-axis −log10 (BH-adjusted p-value). Red, blue, and dark gray dots indicate upregulated, downregulated, and non-significant proteins, respectively. Numbered labels identify selected differentially expressed proteins listed in the tables below each panel.

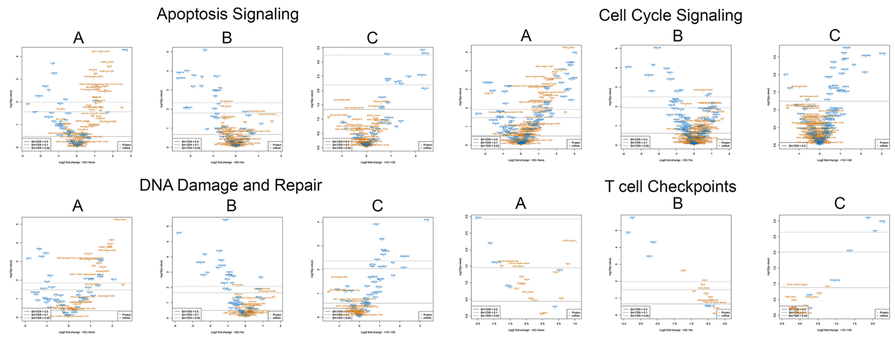

Figure 6. Pathway-focused transcriptomic volcano plots of breast cancers stratified by the abundance of strongly phospho-PERK-positive cells. Differentially expressed genes are shown for four NanoString-defined pathways/processes selected from the 23 analyzed: apoptosis, DNA damage and repair, cell cycle, and T-cell checkpoints. The x-axis represents log2 fold change and the y-axis −log10(BH-adjusted p-value). Horizontal lines indicate BH FDR thresholds.

Acknowledgements

We thank the USA Health Biobank and Histology Core Facility team — Dr. Elba Turbat-Herrera, Dr. Veronica Ramirez-Alcantara, and Terry Pierse — for their technical assistance with immunohistochemistry. We are grateful to Adrian Hoff for his kind assistance in preparing the poster. **This study was funded by a grant from the Breast Cancer Research Foundation of Alabama (BCRFA) to LPY.**

References

1. Fan P, Jordan VC: Estrogen Receptor and the Unfolded Protein Response: Double-Edged Swords in Therapy for Estrogen Receptor-Positive Breast Cancer. Target Oncol 2022, 17(2):111-124.

2. Li C, Fan Q, Quan H, Nie M, Luo Y, Wang L: The three branches of the unfolded protein response exhibit differential significance in breast cancer growth and stemness. Exp Cell Res 2018, 367(2):170-185.

3. Flindris S, Markozannes G, Margioula-Siarkou C, Tsiaras N, Margioula-Siarkou G, Chalitsios C, Sakellariou E, Flindris K, Styliara E, Paschopoulos M et al: Immunohistochemical Expression of IRE1 and PERK in Breast Cancer: Associations With Clinicopathological Characteristics and Survival Outcomes. Cancer Diagn Progn 2025, 5(4):515-529.

4. Kim JY, Heo SH, Song IH, Park IA, Kim YA, Gong G, Lee HJ: Activation of the PERK-eIF2alpha Pathway Is Associated with Tumor-infiltrating Lymphocytes in HER2-Positive Breast Cancer. Anticancer Res 2016, 36(6):2705-2711.

5. Nagelkerke A, Bussink J, Mujcic H, Wouters BG, Lehmann S, Sweep FC, Span PN: Hypoxia stimulates migration of breast cancer cells via the PERK/ATF4/LAMP3-arm of the unfolded protein response. Breast Cancer Res 2013, 15(1):R2.

UNIVERSITY OF SOUTH ALABAMA
COLLEGE OF MEDICINE
CENTER FOR HEALTHY COMMUNITIES

AACR ANNUAL MEETING 2026
April 17 - 22, 2026
San Diego Convention Center
San Diego, California